Clin. Phys. Physiol. Meas., 1991, Vol. 12, No. 3, 253–260. Printed in the UK

An *in vivo* area meter for real-time measurement of cross-sectional area in the cardiovascular system

Kouichi Tamiya†, Masafumi Higashidate‡ and Toshiyuki Beppu†

Departments of †Cardiovascular Science, and ‡Paediatric Cardiovascular Surgery, The Heart Institute of Japan, Tokyo Women's Medical College, 8-1 Kawadacho, Shinjuku-ku, Tokyo 162, Japan

Received 1 November 1990, in final form 11 March 1991

Abstract. A direct real-time recording of the cross-sectional area of the heart valve is useful for the fluid dynamic study of the cardiovascular system. Electronic circuitry is described that is capable of driving the transmitter coil assembly placed outside the animal and detecting an area-related signal induced in the one-turn coil *in vivo*. When a piece of fine pliable metal thread encircles the area of interest (e.g. the mitral/aortic valve orifice) so as to form a single loop, the electrical potential between the ends of the loop is linearly related to the size of the area irrespective of its shape. The principle of measurement, construction of transmitter coil assembly, and simple but accurate direct calibration are also described.

1. Introduction

Although ingenious fluid mechanical models of cardiac valve motion (Henderson and Johnson 1912, Bellhouse and Talbot 1969, Lee and Talbot 1979) have been proposed, instantaneous changes in actual valve opening area of the living animal have not been directly recorded. The mitral valve orifice and anulus areas were measured on the cine x-ray films by suturing multiple radio-opaque markers (Tsakiris *et al* 1975). The aortic valve orifice area was measured on the photo pictures taken while the blood was tentatively replaced with a transparent fluid (van Steenhoven *et al* 1981). A common disadvantage of these visualisation techniques is that the area has to be calculated off-line on the two-dimensional projections.

Recently, we developed a measuring system suitable for real-time area measurement in an animal experiment. The system consists of magnetic field generators for the excitation of the single loop coil implanted in the animal and lock-in amplifiers for the discrimination of the area-related signal from other uncorrelated interfering signals. Since feasibility of the present area meter has already been shown in previous reports (Tamiya *et al* 1986, 1989, Akiyama *et al* 1988, Higashidate *et al* 1988), the present report describes the principle of the *in vivo* area meter, details of the device design, and how to construct the area meter in an ordinary electronics workshop.

2. Measurement system

2.1. Principle of measurement

The configuration of the external drive coils energised by alternating current and a conductive loop sutured along the margin of the aortic valve cusps, as shown in figure 1, is equivalent to a transformer. The extracorporeal drive coils are the primary windings and

0143-0815/91/030253 + 08 $02.50

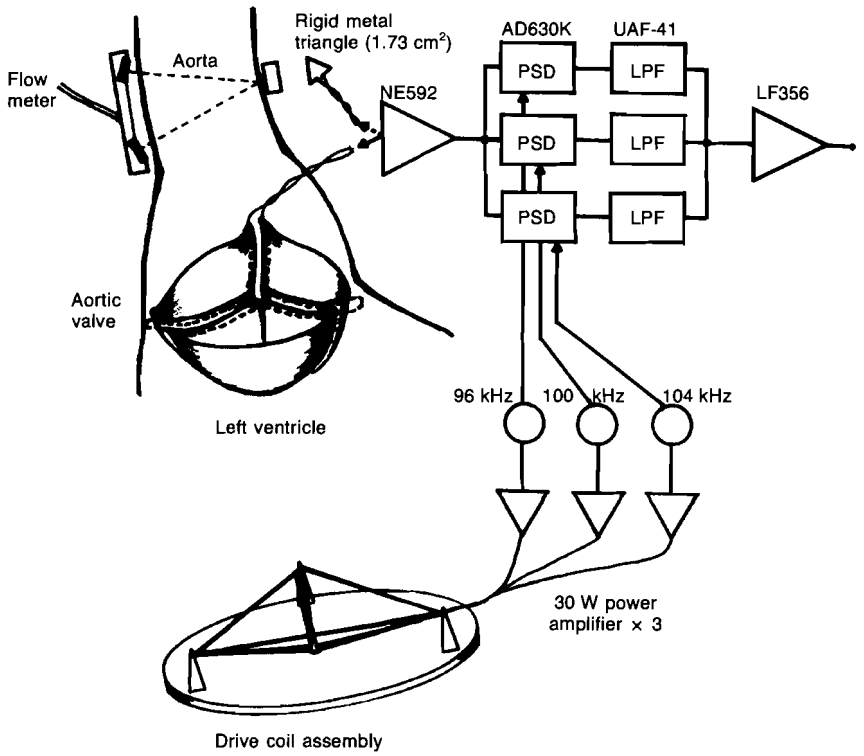

Figure 1. Conceptual drawing of the area meter for aortic valve orifice area measurement. PSD, phase sensitive detector; LPF, low-pass filter.

the *in vivo* metal thread loop is a one-turn secondary. An electromotive force V_t (transformer component) induced in the loop by the alternating magnetic field B is given by

$$V_t = 10^{-8} A \, (dB/dt) \tag{1}$$

where V_t is measured in volts, B in gauss, t in seconds, and loop area A in cm^2. Since the magnetic field is sinusoidal

$$B = B_0 \sin(2\pi ft) \tag{2}$$

where B_0 is the magnetic flux density in gauss, f being the alternating frequency in hertz. Hence the transformer component V_t induced in the secondary winding is proportional to both the frequency f and the projection area A of the secondary loop, and is written as

$$V_t = 10^{-8} \, 2\pi f A B_0 \cos(2\pi ft) \tag{3}$$

If the intensity and frequency of the magnetic field, and the distance between the sensing loop and drive coils are kept constant, the electric potential evoked in the sensing loop is proportional to its loop area A irrespective of its shape.

In practice, however, the total evoked potential consists of two components because of the small fluctuation of the distance between the two windings associated with the heart beat. One has been discussed above as V_t, and the other relates to the moving velocity of the coil in the magnetic field. When a conductive material moves through a magnetic field so as to cut the magnetic flux, an electromotive force generated in the conductor is

proportional to the product of the transverse velocity of the conductor across the magnetic flux and the magnetic flux density itself. The velocity related component V_f is written as

$$V_f = 10^{-8} lvB \tag{4}$$

where V_f is in volts, l is the length of the conductor in cm, v is velocity in cm s^{-1}, and B is in gauss. In an electromagnetic flowmeter, V_f is referred to as a flow component and V_t as a transformer component, v as flow rate, and l as a blood vessel diameter. According to equation (2), V_f is written as

$$V_f = 10^{-8} lvB_0 \sin(2\pi ft) \tag{5}$$

Hence, the total electromotive force $V_f + V_t$ evoked in the one-turn coil is written as

$$V_f + V_t = 10^{-8} B_0 [lv\sin(2\pi ft) + 2\pi fA \cos(2\pi ft)] \tag{6}$$

From equation (6), the wire speed related component V_f is in phase with the ambient magnetic flux density (hence the current through the transmitter coil), and the area related signal V_t is 90° out of phase with the magnetic field intensity. It is also predictable that the higher the frequency of the alternating magnetic field f, the stronger the area proportional signal V_t will be. Since high frequency electromagnetic fields cannot penetrate into a conductive liquid (blood or physiological saline), we chose three frequencies around 100 kHz where the attenuation in the conductive liquid is negligible in the present study. When a conductive loop moves without deformation, the wire speed related signals V_f cancel each other in the loop. Even if the wire loop changes its shape during the cardiac cycle, the phase sensitive detector or 4-quadrant analogue multiplier will effectively segregate the desired area signal from other interfering signals.

In this argument, two planes containing transmitter coil (primary winding) and receiver coil (secondary winding) are assumed to be parallel. In practice, however, a valve axis is assumed to deviate in association with the heart beat. In the present system, a three transmitter coil system was adopted: the axes of the coils are directed toward the sense loop at 20° to the vertical in each case, to reduce the error caused by the phasic sense loop axis deviation relative to the magnetic field.

2.2. Circuit description

2.2.1. Transmitter section. The transmitter consists of three quadrature oscillators which generate 96, 100, and 104 kHz sine/cosine waves and modified three-channel audio power amplifiers which have power handling capability over a frequency of 100 kHz for energising the field coil assembly. VR1 through VR3 (figure 2) should be adjusted to obtain minimum distortion while maintaining stable oscillation. Each cosine wave from the quadrature oscillator is supplied for the corresponding synchronous demodulator (AD630KN, Analog Devices) through the adjustable phase delay circuit (IC5). Three power amplifiers provide about 30 W sine waves for each 25 turn field coil made of 0.5 mm diameter enamel coated copper wire.

2.2.2. Receiver section. A preamplifier, (a high frequency operational amplifier, IC1) amplifies an induced potential 400 times. The differential amplifier (IC2) converts the balanced output from IC1 to single ended and drives the phase sensitive detector (AD630KN) with its low impedance output. Each phase sensitive detector is also fed with an appropriate reference signal supplied directly from the corresponding oscillator in the transmitter section, so that only the 90° out of phase signal (area related signal V_t) is

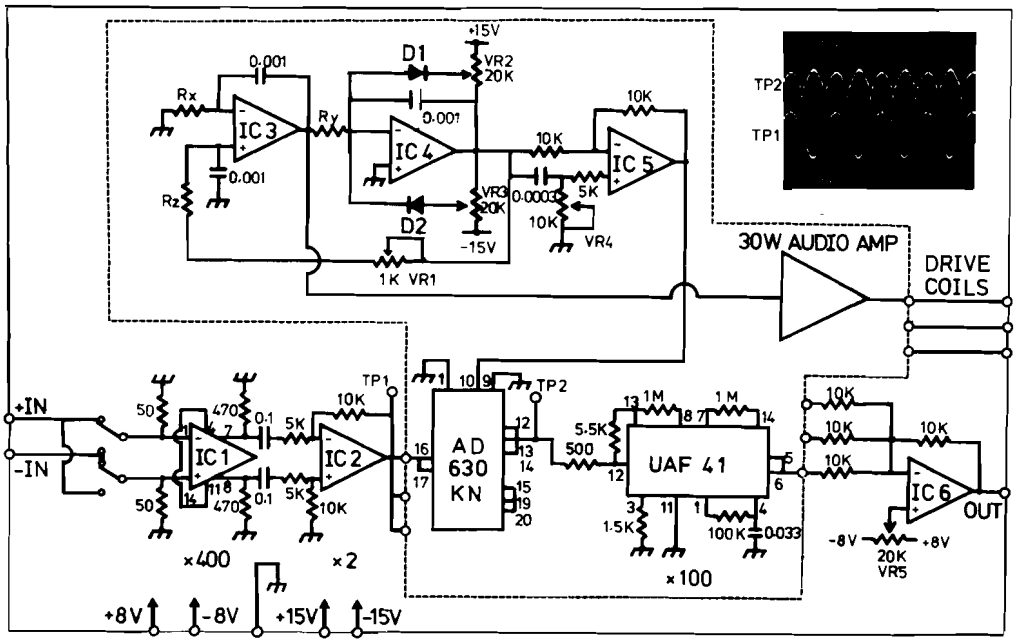

Figure 2. Circuit diagram of the area meter. Two additional sets of the lock-in amplifier section (encircled with broken line) are not shown. Resistor values are expressed in Ω, capacitor values in μF. Rx = Ry = Rz = 1.47 kΩ for 104 kHz, 1.58 kΩ for 100 kHz, 1.65 kΩ for 96 kHz. Bypass capacitors in the power lines are not shown. The upper right panel shows waveforms observed at TP1 and TP2. IC1, NE592; IC2 through IC6, LF356.

discriminated. The adjustable phase sifter (IC5) absorbs phase rotation both in the phase sensitive detector and the audio power amplifier. Thus the combination of the phase sensitive detector (AD630KN) and the low-pass filter (UAF41, Burr Brown) of 50 Hz cut-off frequency compose a lock-in amplifier, which acts as a combined detector and a narrow band-pass filter having an uncorrelated noise rejection ability. The cut-off frequency of the low-pass filter was chosen under the assumption that the valve orifice signal intensity above the 10th harmonics would be negligible (fundamental frequency is a heart rate). The final stage (IC6) adjusts DC offset and averages three outputs of different frequency. The phase delay was adjusted by VR4 so that the simultaneous oscilloscope traces at TP1 and TP2 look like those shown in the right upper panel of figure 2, while the rigid triangle of fixed area for calibration is connected and held stationary in the magnetic field. We observed 1 V output for a 1.73 cm^2 loop with × 80000 (98.1 dB) amplification when the distance between the sensor and the drive coils were set at about 120 cm. The sensitivity of the present system was therefore estimated to be 7.2 $\mu V\ cm^{-2}$. To adjust the zero offset, a zero area signal could be input by detaching the sensing loop and shunting the preamplifier input. Preamplifier input shunting without detaching the probe does not give an adequate zero area signal because of the extremely low source impedance of the probe (impedance of the one-turn coil).

3. *In vitro* calibration

The drive coil assembly containing three transmitter coils is located approximately 1.2 m away from the sensing loop so that the magnetic field focuses on the area of interest. As the first order approximation, 1 cm fluctuation of the distance between the transmitter coil

assembly and the sensing loop causes a 0.83% area signal error at most. The structure of the drive coil assembly, whose axes intersect with each other at vertically opposite angles of 20°, is shown in figure 3(*a*). When the rigid triangle, made of three 2 cm long brass rods (area = 1.73 cm^2), is placed parallel to the transmitter coil base at the same distance as that of the sensing loop, the output gives the standard reference area signal of 1.73 cm^2.

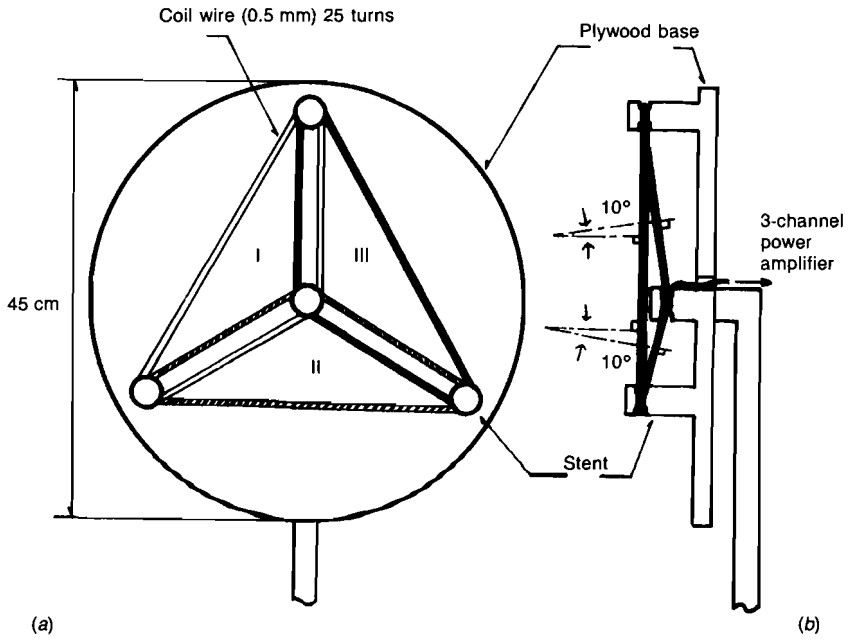

Figure 3. Schematic drawing of the transmitter coil assembly. (*a*) front view, (*b*) side view. I (open line), II (slashed line), III (solid line) denote three individual coils whose axes intersect with each other at vertically opposite angles of 20°.

Parallel bars at 1 cm separation were mounted on an acrylic resin board: one end of each bar was connected to the area meter, as shown in the inset of figure 4(*a*). By sliding a metal bar that shunts the parallel bars at a desired position, we could provide a variable standard signal of known area for the area meter. The relation between the area enclosed by the metal rods and the output is shown in figure 4(*a*). The effect of three-signal averaging was evaluated at various receiver loop angles. In figure 4(*b*), open circles denote the outputs of the three-frequency carrier system. Closed circles denote the output of a single transmitter-receiver pair. According to figure 4(*b*) changes in the angle within ±25° produces tolerable error in the three drive coil system, while only ±15° deviation is tolerable in a single carrier system. The alteration of output from 1.38 to 1.41 V was observed when the insulated rigid metal loop of area 4 cm^2 was immersed in 1000 ml of physiological saline. The change is so small compared with the signal intensity, we concluded that the effect of the ambient medium conductivity was negligible around the frequency of 100 kHz.

4. *In vivo* application

For the *in vivo* application, the receiver loop was made of stranded urethane-resin coated copper wires (four 25 μm diameter Uremett wire, Sumitomo Denko). The metal thread was

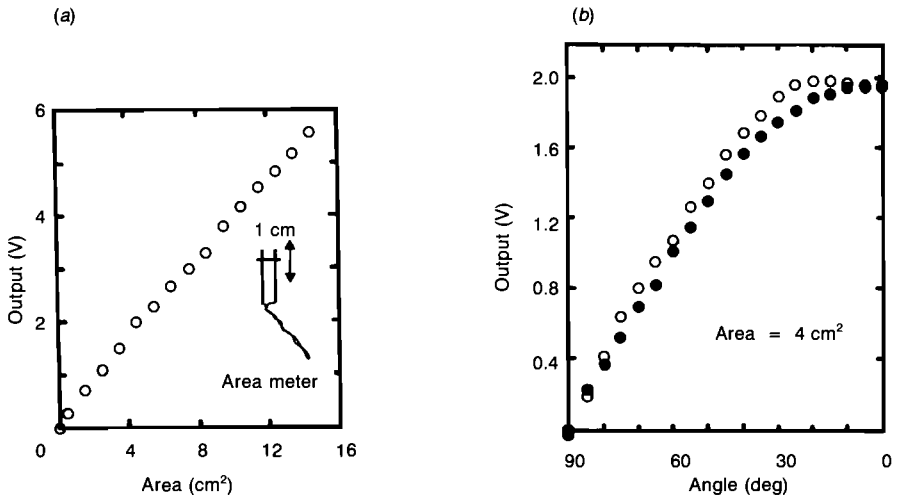

Figure 4. (*a*) Relation between the area and the output in the air. $Y = 0.13 + 0.38x$. $R = 0.99$. Parallel bars with a sliding short circuit bar shown in the inset provide various area signals for the area meter. (*b*)The effect of the plane rotation on the output for the same area in the triple carrier system (open circles) and the single carrier system (closed circles). The abscissa denotes angles between the axis of the drive coil base and that of the sensing loop. The distance between drive coil assembly and the sensing loop was 120 cm. Area of the sensing loop was 4 cm^2.

softly twisted and attached to a surgical needle with cyano-acrylate glue and looking just like a braided silk surgical suture with a non-traumatic needle. Through surgical procedures during extra-corporeal circulation using an artificial heart-lung machine, the valve orifice was encircled by the metal thread with a continuous stitch. Then the sensing loop was connected to the preamplifier with a short segment of shielded twisted pair by soldering, so that an extra loop formation was carefully avoided. Figure 5 shows representative recordings of the output signal obtained from the metal thread loops implanted around the mitral valve orifice (*a*) and aortic valve orifice (*b*) in anaesthetised open-chest dogs. Aortic flow was measured with an ultrasonic transit time flowmeter (model T-102, Transonic Systems, Ithaca, NY). Since the synchronous detector does not eliminate the undesired signal that corresponds to carrier harmonics, a square wave electromagnetic flowmeter may interfere with the area meter when used close to the receiver coil. If this is the case, a narrow band-pass filter between the preamplifier and the demodulator will minimise the interference.

Recently, aortic root deformation during the cardiac cycle was reported using a magnetic induction system (van Renterghem *et al* 1988) or through computer aided video analysis (Vesely *et al* 1990). These methods require complex and expensive equipment. Furthermore, they do not directly measure the area itself, but length between two markers. The present *in vivo* area meter is able to provide on-line phasic variations of the cross-sectional area (e.g. valve orifice area, valve ring area, cross-sectional area of the great vessels) in the cardiovascular system, and causes minimum disturbance to natural valve motion. The present system is simple and inexpensive; however, it could not provide any information on the shape of the area.

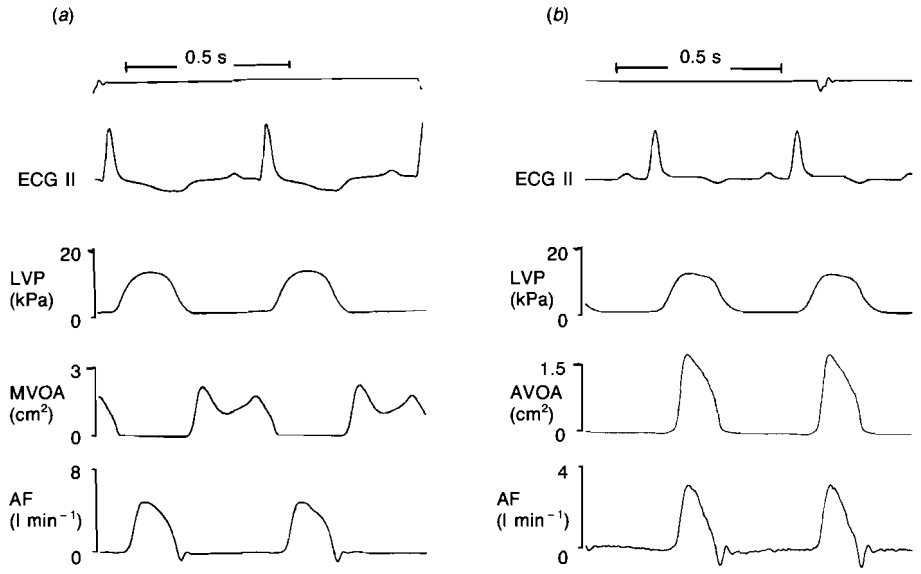

Figure 5. Phasic changes in the mitral valve orifice area (*a*) and that of the aortic valve (*b*) with relevant haemodynamic parameters in the anaesthetised dogs. (*a*) from top; electrocardiogram (ECG II), left ventricular pressure (LVP), mitral valve orifice area (MVOA), and aortic flow (AF) measured with ultrasonic transit time flowmeter. (*b*) MVOA is replaced with aortic valve orifice area (AVOA).

5. Conclusion

The present area meter is very stable and has an appropriate signal-to-noise ratio with controllable frequency response (determined by the low-pass filter employed) and is easy to handle in the animal experiments. The system will be easily fabricated inexpensively with commonly available electronic parts, and should be useful for many biological area measurements.

Acknowledgement

This study was supported in part by grants 01750226, 02750358, 03670467 from the Ministry of Education and Science of Japan, and Open Research Grant 1989 from the Japan Research Promotion Society for Cardiovascular Diseases.

References

Akiyama K, Sawatani O, Imamura E, Koyanagi H, Higashidate M and Tamiya K 1988 *In vitro* analysis of performance of porcine xenografts with inward bending of stent posts: Real-time measurement of valve orifice area using an area meter *Ann. Thorac. Surg.* **46** 331-6

Bellhouse B J and Talbot L 1969 The fluid mechanics of the aortic valve *J. Fluid Mech.* **6** 199-210

Henderson Y and Johnson F E 1912 Two modes of closure of the heart valves *Heart* **4** 69-82

Higashidate M, Tamiya K, Kurosawa H, Takanashi Y and Imai Y 1988 Real-time measurement of tricuspid valve annular area for annuloplasty *J. Thorac. Cardiovasc. Surg.* **96** 88-91

Lee C S F and Talbot L 1979 A fluid-mechanical study of the closure of heart valves *J. Fluid Mech.* **91** 41-63

van Renterghem R J, Arts T, van Steenhoven A A and Reneman R S 1988 On-line measurement of aortic valve ring deformation during the cardiac cycle *Am. J. Physiol.* **254** H795-800

van Steenhoven A A, Verlaan C W J, Veenstra P C and Reneman R S 1981 *In vivo* cinematographic analysis of behavior of the aortic valve *Am. J. Physiol.* **240** H286-92

Tamiya K, Higashidate M and Kikkawa S 1986 Technique with lock-in amplifier for real-time measurement of tricuspid valve annulus area *Am. J. Physiol.* **251** H236-41

——— 1989 Real-time and simultaneous measurement of tricuspid orifice and tricuspid anulus areas in anesthetized dogs *Circ. Res.* **64** 427-36

Tsakiris A G, Gordon D A, Mathieu Y and Lipton I 1975 Motion of both mitral valve leaflets: cineroentgenographic study in intact dogs *J. Appl. Physiol.* **39** 359-66

Vesely I, Menkis A and Campbell G 1990 A computerized system for video analysis of the aortic valve *IEEE Trans. Biomed. Eng.* **BME-10** 925-9